

# A post-processing method for 3D fluorescence microscopy images

Andrey Krylov, Andrey Nasonov, Yakov Pchelintsev and Alexandra Nasonova

*Laboratory of Mathematical Methods of Image Processing*

*Faculty of Computational Mathematics and Cybernetics*

*Lomonosov Moscow State University*

Moscow, Russia

kryl@cs.msu.ru, nasonov@cs.msu.ru

**Abstract**—Three-dimensional (3D) deconvolution microscopy is very effective in improving the quality of fluorescence microscopy images. However, due to ill-posed nature of the deconvolution, many images still remain blurry after deblurring algorithms. We use an edge sharpening algorithm based on pixel grid warping to further improve the quality of blurry images in edge areas. Its main idea is to move pixels toward the nearest image edge to make them sharper without noise amplification. In this paper, we improve the results of recently developed 3D post-processing algorithm by considering the blur kernel that correspond to real optic blur and by optimizing the pixel displacement function. We illustrate its effectiveness on real data with modeled blur.

**Index Terms**—edge sharpening, image deblurring, grid warping, optical blur, 3D image sharpening

## I. INTRODUCTION

Image blur occurs in numerous types of 2D and 3D images, e.g. photographs, medical images of different modalities, telescopes, microscopes, satellite sensors, etc. As a consequence, the deblurring problem (also called deconvolution) is widely investigated for simpler 2D case and then extended to 3D case. Deblurring methods require explicit knowledge or accurate estimation of the blurring kernel — Point Spread Function (PSF).

Image deblurring is a challenging ill-posed problem of finding a sharp image  $I_0$  from the given blurred image  $I_B$  using the blur model

$$I_B = I_0 * H + n.$$

If the blur kernel  $H$  and noise  $n$  are known exactly, the deconvolution problem can be effectively solved by regularization-based algorithms [1].

Typically, there is no or few information about  $H$  and  $n$ . In that case, the blur kernel is to be estimated. There are some fairly powerful techniques for blind image deblurring [2], [3]. Non-uniformity of image blur, noise and blur kernel estimation errors may significantly degrade the result. It is not easy to find optimal parameters for a compromise between smooth result with blurry edges and sharp result with artifacts like ringing or noise amplification when blur kernel is estimated with errors.

Blurred image enhancement methods that are not based on the PSF concept can be referred to as image sharpening

methods. A commonly used method of image sharpening is the unsharp masking method [4], [5]. The main problem of the existing sharpening methods is unwanted overshooting artifact and noise amplification that may appear in the output image [6].

The aim of the paper is to develop a post-processing method to enhance the results of existing image deblurring algorithms. We present an image sharpening method that performs the enhancement of a blurred image in the neighborhood of image edges. The idea is to transform the neighborhood of the blurred edge so that the neighboring pixels move closer to the edge, and then resample the image from the warped grid to the original uniform grid.

The warping approach is related to the morphology-based sharpening [7] and shock filters [8]–[10]. But these methods make the image appear piecewise constant which is effective mostly for cartoon-like images. The proposed method is applied to edges locally so the textures are preserved a priori. Also warping compresses the edge neighborhood at fixed rate and does not make the image piecewise constant.

The warping approach for image enhancement was initially introduced as the solution of a differential equation derived from the warping process constraints [11]. The solution of the equation is used to move the edge neighborhood closer to the edge, and the areas between edges are stretched. The method has several parameters, and the choice of optimal values for the best result is not easy. Due to the global nature of the method the resulting shapes of the edges are often distorted. In another work [12], the warping map is computed directly using the values of left and right derivatives. In both these methods [11], [12] the pixel shifts are proportional to the gradient values. It results in oversharpening of already sharp and high contrast edges and insufficient sharpening of blurry and low contrast edges. Both methods also introduce small local changes in the direction of edges and produce aliasing effect due to calculation of horizontal and vertical warping components separately.

Application of grid warping method for the enhancement of 2D image deblurring methods has been already considered [13], [14]. In this work, we improve the results of recently developed 3D post-processing algorithm [15] by considering the blur kernel that correspond to real optic blur and by

optimizing the pixel displacement function.

## II. VOLUME IMAGE BLUR MODEL

Although 2D PSF of a microscope can be approximated by a Gaussian kernel, 3D PSF does not have an accurate Gaussian approximation [16]. There is a variety of PSF models, but the most popular is the Gibson-Lanni model [17], [18]. This model takes into consideration the difference between the design conditions and experimental conditions, such as the object thickness and coverslips. An example of 3D microscopy PSF based on the Gibson-Lanni model is shown in Fig. 1.

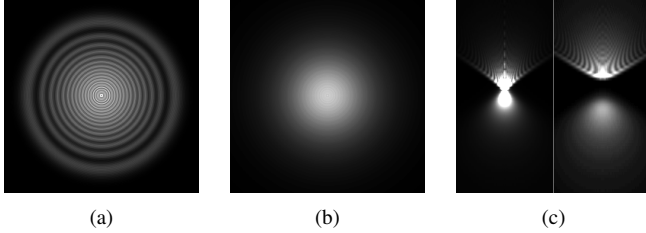


Fig. 1: An example of the 3D microscopy PSF ( $256 \times 256 \times 75$ ) based on the Gibson-Lanni model. a, b) ( $x, y$ ) sections, the 24th and the 44th slices. c) ( $x, z$ ) section, the 127th and the 192nd slices. Here the images are stretched in  $z$  dimension to make the spatial resolution in both  $x$  and  $z$  directions equal.

## III. ONE-DIMENSIONAL EDGE SHARPENING

The idea of the proposed 3D image sharpening algorithm is to move pixels towards edge centerline [19]. Consider one-dimensional edge profile  $g(x)$  centered at the point  $x = 0$  (see Fig. 2),  $d(x)$  — displacement function and  $h(x) = g(x+d(x))$  — warped edge profile.

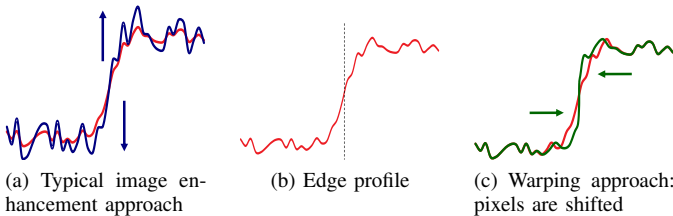


Fig. 2: The idea of edge sharpening using grid warping. Red line is the original edge profile, blue line is the edge profile sharpened using grid warping.

Simple scaling  $f(x) = kx$  will give sharper edge but it will also shrink the entire image. To make the edge sharper without changing image size, only the area near the edge center should be shrunk while the area outside the edge should be stretched proportionally.

The warped grid should remain monotonic (i.e. for any  $x_1 < x_2$  new coordinates should be  $x_1 + d(x_1) \leq x_2 + d(x_2)$ ), so the displacement function should match the following constraint:

$$d'(x) \geq -1. \quad (1)$$

Another constraint localizes the area of warping effect near the edge center:

$$d(x) \rightarrow 0, \quad |x| \rightarrow \infty. \quad (2)$$

The displacement function  $d(x)$  greatly influences the result of the edge warping. On the one hand, the edge slope should become steeper. On the other hand, the area near the edge should not be stretched over some predefined limit to avoid wide gaps between adjacent pixels in the discrete case.

The work [19] constructs the displacement function  $d(x)$  using the proximity function

$$p(x) = 1 + d'(x)$$

$$d(x) = \int_{-\infty}^x (p(y) - 1) dy. \quad (3)$$

The proximity is the distance between adjacent pixels after image warping. This value is inverse to the density value. If the proximity function  $p(x)$  is less than 1, then the image area is shrunk at the coordinate  $x$ . If the proximity is greater than 1, then the image is stretched. The identity transform has the value  $p(x) \equiv 1$ .

The constraint (1) leads to non-negativity of the proximity function. Also high values of the proximity function should be avoided to preserve image textures.

## IV. VOLUMETRIC IMAGE SHARPENING

To apply the warping algorithm to 3D images, we generalize the two-dimensional extension [19] to the three-dimensional case. The displacement is a 3D vector field  $\vec{d}(x, y, z)$  with the following constraints similar to the 2D case:

1) The shapes of the edges cannot be warped, so  $\vec{d}(x_e, y_e, z_e) = 0$  for each edge point  $(x_e, y_e, z_e)$ .

2) There cannot be any turbulence:  $\text{rot } \vec{d} = 0$ . Since  $\text{rot } \nabla u \equiv 0$ , the displacement field is assumed to be gradient of some scalar function  $u(x, y, z)$ :  $\vec{d}(x, y, z) = \nabla u(x, y, z)$ .

3) The constraint (1) takes the form

$$\text{div } \vec{d} \geq -1 \quad (4)$$

and the proximity function is

$$p(x, y, z) = 1 + \text{div } \vec{d}(x, y, z). \quad (5)$$

Since  $\text{div } \nabla \equiv \Delta$ , where  $\Delta$  is a Laplacian, the warping problem is posed as a Dirichlet problem for the Poisson equation in the area of the image:

$$\begin{cases} \Delta u & = p(x, y, z) - 1, \\ u(x, y, z) & = 0 \text{ at image borders.} \end{cases} \quad (6)$$

The second constraint here is the boundary condition: the displacements at image borders should be equal to zero.

In order to get the same results as in the 1D case and to keep the edge pixels unwrapped, the proximity value should be equal to the 1D proximity function depending on the distance to the edge. However, the distance to the closest edge  $\rho$  as an argument of the proximity function  $p(\rho)$  is not efficient as

it may produce gaps between close edges. Also it blurs edge ends.

We suggest the following method for calculating the proximity function:

$$p(x_0, y_0, z_0) = \frac{\sum_{(x,y,z) \in E(x_0, y_0, z_0)} p(x_n) G_\sigma(x_t) |\vec{g}(x, y, z)|}{\sum_{(x,y,z) \in E(x_0, y_0, z_0)} |\vec{g}(x, y, z)|} \quad (7)$$

where  $E(x_0, y_0, z_0)$  is the set of edge points in the neighborhood of  $(x_0, y_0, z_0)$ . The 3D edge point set is obtained using 3D Canny edge detector which is similar to 2D algorithm [20].

The value  $x_n$  is the projection and the value  $x_t$  is the length of the rejection of the vector  $(x_0 - x, y_0 - y, z_0 - z)$  on the edge gradient vector  $\vec{g}(x, y, z)$ .

The function  $p(x_n)$  is the 1D proximity function, weighting function  $G_\sigma(x_t)$  is Gauss function with standard deviation equal to the edge's blur  $\sigma$ .

We solve the partial differential equation (6) using Fourier transform technique.

## V. PROXIMITY FUNCTION MODELS

Two models have been considered for the choice of the proximity function.

### A. Difference of Gaussian functions

For volumetric Gaussian blur with parameter  $\sigma$ , the difference of two Gaussian functions is used as a proximity function [15]:

$$p_1(x) = 1 + \kappa(G_{\sigma_1}(x) - G_{\sigma_2}(x)), \quad \sigma_2 > \sigma_1, \quad (8)$$

$$\kappa = 1 / (G_{\sigma_1}(0) - G_{\sigma_2}(0)).$$

It allows to control the areas of shrinkage and stretching independently [19]. Parameter  $\sigma_1$  controls the width of the densification area while parameter  $\sigma_2$  controls the width of the rarefaction area. We use  $\sigma_1 = \sigma$  and  $\sigma_2 = 2\sigma$ . Fig. 3 illustrates grid warping for edge sharpening using this proximity function.

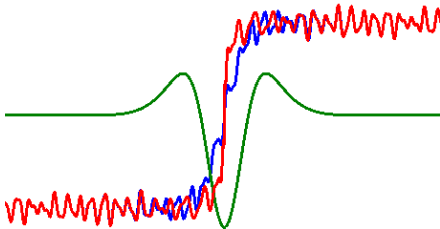


Fig. 3: Edge sharpening by grid warping using the proximity function (8). Blue function is the blurred edge with some noise. Red function is the result of warping. Green line is the proximity function.

### B. Piecewise constant

In piecewise constant model (PWC), the area of densification with constant parameter is followed by the area of rarefaction with another constant parameter [21]:

$$p_2(x)[a, b, c] = \begin{cases} 1 + \frac{c}{a}, & |x| \leq a, \\ 1 - \frac{c}{b-a}, & a < |x| \leq b, \\ 1, & |x| > b. \end{cases}$$

The corresponding 1D displacement function looks as:

$$d_2(x)[a, b, c] = \begin{cases} \frac{c}{a}x, & |x| \leq a, \\ c \frac{b-|x|}{b-a} \text{sign } x, & a < |x| \leq b, \\ 0, & |x| > b. \end{cases}$$

Despite the discontinuities, this model has greater sharpening effect than DoG model (8).

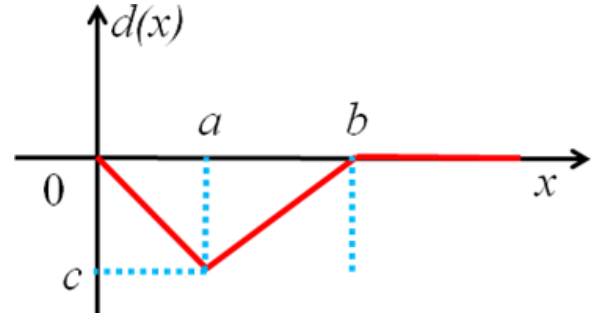


Fig. 4: Piecewise linear displacement function.

The parameters  $a$ ,  $b$  and  $c$  define the width of densification and rarefaction areas and the steepness of the displacement function. The plot of this displacement function can be seen at Fig. 4. The strongest warping effect which meets the condition (1) is achieved when  $c = -a$ . Therefore, we use the proximity function with two parameters:

$$p_2(x)[a, b] = p_2(x)[a, b, -a] = \begin{cases} 0, & |x| \leq a, \\ \frac{b}{b-a}, & a < |x| \leq b, \\ 1, & |x| > b. \end{cases} \quad (9)$$

During the experiments we analyzed the choice of parameters  $a$  and  $b$  in order to maximize objective image quality. It was found that the ratio  $b/a$  of optimal parameters  $a$  and  $b$  was different for different images. At the same time, variations of the parameter  $b$  did not significantly influence the image quality. To reduce the number of parameters at the cost of insignificant decrease of image quality, we set  $b = \frac{3}{2}a$ :

$$p_2(x)[a] = p_2(x)[a, \frac{3}{2}a, -a] = \begin{cases} 0, & |x| \leq a, \\ 3, & a < |x| \leq \frac{3}{2}a, \\ 1, & |x| > \frac{3}{2}a. \end{cases} \quad (10)$$

## VI. RESULTS

Test 3D images were generated using *Pollen* image, which is a thin optical section through the center of the desiccated stage of the mature pollen, collected from <http://www.cellimagelibrary.org/images/35532>. 16-bit reference image was convolved with the Gibson-Lanny blur kernel and corrupted by Poisson noise with different noise levels  $\lambda$ . Then Richardson-Lucy algorithm [22], [23] with Total-Variation regularization [24] and 200 iterations was applied to restore the original image from the convolution result. ImageJ software with plugin DeconvolutionLab2 was used. The examples of images are at Fig. 5.

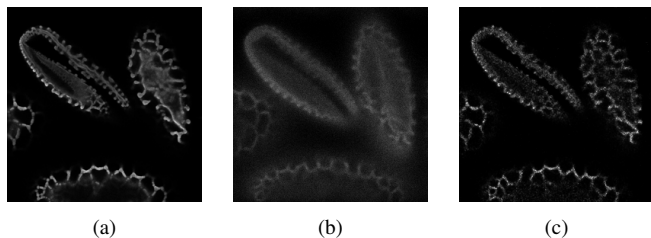


Fig. 5: An example of the test image set,  $(x, y)$  section. a) Reference image. b) Blurred and noisy image. c) Deblurred image using RL-TV [24] method.

Then we applied image warping with two considered models as a post-processing algorithm after image deblurring. The results are shown in Table I and Figures 6, 7.

The execution time of image warping algorithm for  $256 \times 256 \times 75$  image is about 50 seconds for Intel Core i5 Skylake processor, and 5 minutes for  $1024 \times 1024 \times 75$  image. RL-TV algorithm from DeconvolutionLab2 plugin has taken 8 minutes and 10 hours respectively. Fast GPU implementation of the proposed algorithm is possible [25].

Method	No noise	$\lambda = 15$	$\lambda = 50$
Blurred and noisy images	27.05	27.05	27.04
RL-TV [24]	32.16	32.08	29.99
RL-TV + DoG warping (8)	32.20	32.13	30.21
RL-TV + PWC warping (10)	32.30	32.24	30.37

TABLE I: PSNR values for test image deblurring with different noise levels and different warping proximity function.

## VII. CONCLUSION

The proposed method sharpens 3D images in edge areas. It has the following advantages and features:

1. The best results are achieved when grid warping is used as a post-processing method after deconvolution-based image deblurring methods. Traditional image deblurring methods improve overall image quality while grid warping pays special attention to image edges.

2. No artifacts like ringing effect or noise amplification are introduced because pixel values are not changed.

3. Unlike morphological methods and shock filters, the resulting images look natural and do not inevitably become piecewise constant.

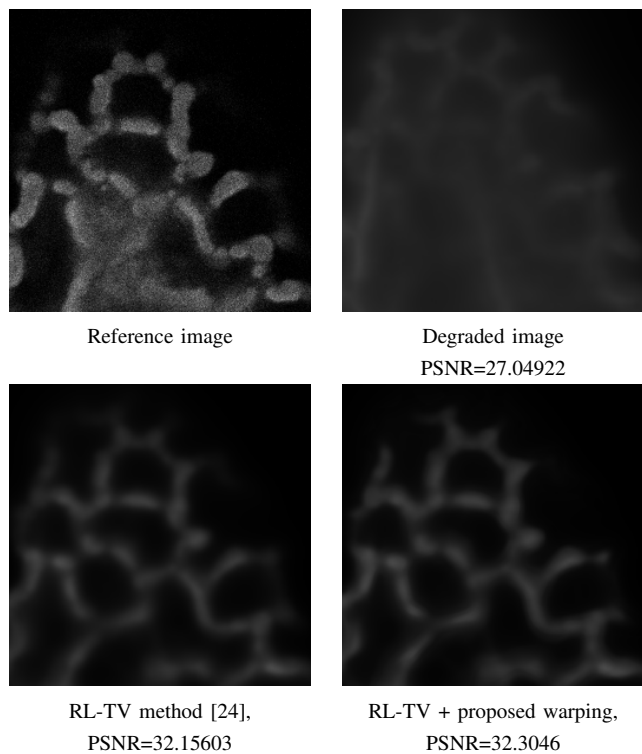


Fig. 6: Image warping algorithm example 1, PWC proximity function model (10),  $a = 0.67$ .

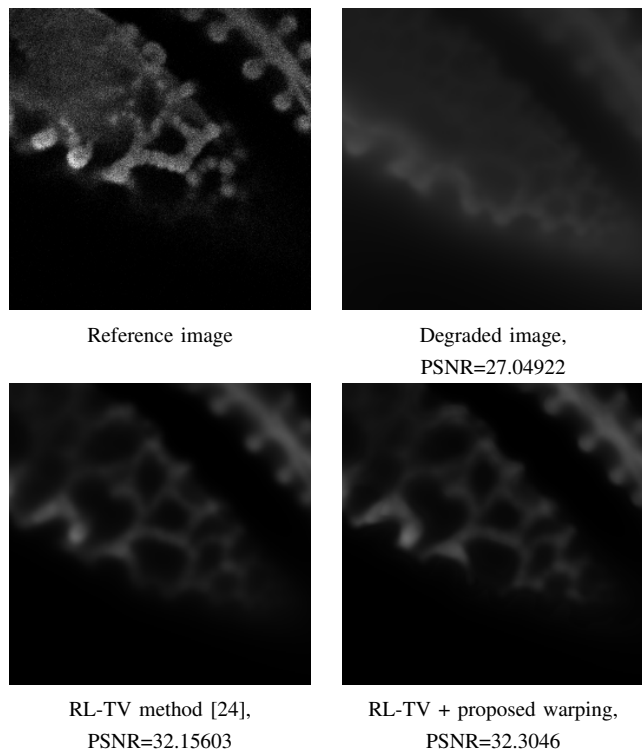


Fig. 7: Image warping algorithm example 2, PWC proximity function model (10),  $a = 0.67$ .

## REFERENCES

- [1] J. Oliveira, J. M. Bioucas-Dia, and M. Figueiredo, "Adaptive total variation image deblurring: A majorization-minimization approach," *Signal Processing*, vol. 89, pp. 1683–1693, 2009.
- [2] M. Almeida and M. Figueiredo, "Parameter estimation for blind and non-blind deblurring using residual whiteness measures," *IEEE Transactions on Image Processing*, vol. 22, pp. 2751–2763, 2013.
- [3] S. D. Babacan, R. Molina, and A. K. Katsaggelos, "Variational bayesian blind deconvolution using a total variation prior," *IEEE Transactions on Image Processing*, vol. 18, pp. 12–26, 2009.
- [4] G. Ramponi, "A cubic unsharp masking technique for contrast enhancement," *Signal Processing*, vol. 67, pp. 211–222, 1998.
- [5] G. Ramponi, N. Strobel, S. Mitra, and T. Yu, "Nonlinear unsharp masking methods for image contrast enhancement," *Journal of Electronic Imaging*, vol. 5, pp. 353–366, 1996.
- [6] Z. Gui and Y. Liu, "An image sharpening algorithm based on fuzzy logic," *Optik - International Journal for Light and Electron Optics*, vol. 122, no. 8, pp. 697–702, 2011.
- [7] J. Schavemaker, M. Reinders, J. Gerbrands, and E. Backer, "Image sharpening by morphological filtering," *Pattern Recognition*, vol. 33, no. 6, pp. 997–1012, 2000.
- [8] S. Osher and L. I. Rudin, "Feature-oriented image enhancement using shock filters," *SIAM Journal on Numerical Analysis*, vol. 27, no. 4, pp. 919–940, 1999.
- [9] G. Gilboa, N. A. Sochen, and Y. Y. Zeevi, "Regularized shock filters and complex diffusion," *Lecture Notes in Computer Science*, vol. 2350, pp. 399–413, 2002.
- [10] J. Weickert, "Coherence-enhancing shock filters," *Lecture Notes in Computer Science*, vol. 2781, pp. 1–8, 2003.
- [11] N. Arad and C. Gotsman, "Enhancement by image-dependent warping," *IEEE Transactions on Image Processing*, vol. 8, pp. 1063–1074, 1999.
- [12] J. Prades-Nebot et al., "Image enhancement using warping technique," *IEEE Electronics Letters*, vol. 39, pp. 32–33, 2003.
- [13] A. Krylov, A. Nasonova, and A. Nasonov, "Image warping as an image enhancement post-processing tool," *OGRW2014*, pp. 132–135, 2015.
- [14] A. S. Krylov, A. V. Nasonov, A. V. Razgulin, and T. E. Romanenko, "A post-processing method for 3d fundus image enhancement," in *International Conference on Signal Processing (ICSP2016)*, Chengdu, China, 2016, pp. 49–52.
- [15] A. Krylov, A. Nasonov, A. Razgulin, and T. Romanenko, "A post-processing method for 3d fundus image enhancement," in *Signal Processing (ICSP), 2016 IEEE 13th International Conference on*. IEEE, 2016, pp. 49–52.
- [16] B. Zhang, J. Zerubia, and J.-C. Olivo-Marin, "Gaussian approximations of fluorescence microscope point-spread function models," *Applied Optics*, vol. 46, no. 10, pp. 1819–1829, 2007.
- [17] J. Li, F. Luisier, and T. Blu, "Pure-let deconvolution of 3d fluorescence microscopy images," in *Proceedings of IEEE International Symposium on Biomedical Imaging (IEEE, 2017)*, (to be published), 2017.
- [18] S. F. Gibson and F. Lanni, "Experimental test of an analytical model of aberration in an oil-immersion objective lens used in three-dimensional light microscopy," *JOSA A*, vol. 8, no. 10, pp. 1601–1613, 1991.
- [19] A. Nasonova and A. Krylov, "Deblurred images post-processing by poisson warping," *IEEE Signal Processing Letters*, vol. 22, no. 4, pp. 417–420, 2015.
- [20] J. Canny, "A computational approach to edge detection," *IEEE Trans. Pattern Analysis and Machine Intelligence*, vol. 8, pp. 679–698, 1986.
- [21] Y. P. Andrey Krylov, Andrey Nasonov, "Single parameter post-processing method for image deblurring," *International Conference on Image Processing Theory, Tools and Applications (IPTA 2017)*, 2017.
- [22] W. H. Richardson, "Bayesian-based iterative method of image restoration," *JOSA*, vol. 62, no. 1, pp. 55–59, 1972.
- [23] L. B. Lucy, "An iterative technique for the rectification of observed distributions," *The astronomical journal*, vol. 79, p. 745, 1974.
- [24] N. Dey, L. Blanc-Feraud, C. Zimmer, P. Roux, Z. Kam, J.-C. Olivo-Marin, and J. Zerubia, "Richardson-lucy algorithm with total variation regularization for 3d confocal microscope deconvolution," *Microscopy research and technique*, vol. 69, no. 4, pp. 260–266, 2006.
- [25] A. D. Gusev, A. V. Nasonov, and A. S. Krylov, "Parallel implementation of image sharpening method using grid warping," *Proceedings of the 26th International Conference on Computer Graphics and Vision GraphiCon'2016*, pp. 294–297, 2016.